Dust Structure Around White Dwaf WD 1003-44 in 60 & 100 μm Iras Survey

Binil Aryal[1] & Ronald Weinberger[2]
[1]*Central Department of Physics, Tribhuvan University, Kirtipur, Nepal*
[2]*Institute of Astro- and Particle Physics, Innsbruck University, Innsbruck, Austria*
binil.aryal@uibk.ac.at

Abstract

We studied the dust structures in 100 micron infrared image around the white dwarf WD 1003-441. The post Asymptotic Giant Branch (AGB) emission of the white dwarf's precursors' wind and the ambient interstellar matter is studied. For this, distribution of the relative flux density is studied and analyzed in the context of the dust color temperature, mass loading trend and the amount of total mass deposited due the interaction in the interstellar medium. The 100 micron far-infrared image is provided by the Groningen server of Infrared Astronomical Satellite (IRAS) survey. The curved emission structure at 100 micron in the region of interest is probably due to the interaction between the ambient interstellar medium and the He-flashes of the parent planetary nebula of the central white dwarf WD 1003-441. This white dwarf is a PG1159 star with 9-11 detected periods and an associated planetary nebula mass ejection. The total mass of the filamentary arc is found to be ~ 8 x 10^{-2} solar masses, as predicted. The mass loss rate of the post AGB star goes up to 10^{-5} solar masses per year. It is concluded that the first He-flash occurred at least ~1000 years ago. The amount of total mass around this white dwarf is about ~ 0.134 solar mass. The maximum and minimum dust color temperature around the white dwarf is found to be 19.0 K (±1.5 K) and 22.0 K (±2.0 K), respectively.

Key-Words: white dwarf – interstellar medium – flux density – interstellar dust – mass of the gas

1   INTRODUCTION

The Asymptotic Giant Branch is the name given to a region of the Hertzsprung-Russell diagram populated by evolving low to medium-mass stars. When a star exhausts the supply of hydrogen in its core, the core contracts and its temperature increases, causing the outer layers of the star to expand and cool. The star's luminosity increases greatly, and it becomes a red giant, following a track leading into the upper-right hand corner of the HR diagram (Blandford & Rees, 1974). The AGB phase is divided into two parts, the early AGB (E-AGB) and the thermally pulsing AGB (TP-AGB). During the E-AGB phase the main source of energy is helium fusion in a shell around a core consisting mostly of carbon and oxygen. During this phase the star swells up to giant proportions to become a red giant again. The star may become as large as one astronomical unit. After the helium shell runs out of fuel, the TP-AGB starts. Now the star derives its energy from fusion of hydrogen in a thin shell, inside of which lies in the now inactive helium shell. However, on periods of 10,000 to 100,000 years the helium shell switches on again, and the hydrogen shells switches of, a process known as a helium shell flash (Cox, 2005).

Towards the finale of their lifetime, almost all (95-98%) stars, that is stars of low and intermediate initial mass (~1-8 solar masses) lose a substantial fraction of their mass on the Asymptotic Giant Branch (AGB) in form of massive winds, which compels them into the Planetary Nebula (PN) phase (Rees, 1984). The central star of PN is the white dwarf. The massive stellar wind emitted from the AGB star interacts with the ambient interstellar medium. Thus the structure (gas or the dust) around the white dwarf preserve the history as a fossil record of the early and late AGB phase of the star. It is important to understand the shaping process of interstellar clouds as well as the nature of the emission from AGB to PN phase. The white dwarf is suspected to reside within giant dust structures which may represent fossil records of its progenitor's transition from spherically symmetric to bipolar or unipolar mass loss (Aryal & Weinberger, 2006; Aryal, Rajbahak & Weinberger, 2010). It can be suspected that the white dwarf is not the only one where fossil records of ancient mass loss in its neighborhood as well as signs of the resulting shaping can be traced. Besides being ideal laboratories for the study of various astrophysical processes prevailing in highly excited dilute nebulae, PNe and their progenitors are key objects for the understanding of the evolution of stars. In this connection,

the transformation from spherically symmetric AGB winds to non-spherical PNe represents one of the most enduring problems of stellar astrophysics (e.g. Aryal, Rajbahak & Weinberger, 2009; Balick, 2002).

In this work we present a detailed study of dust structures around white dwarf WD 1003-44 in order to understand the fossil records of its evolution during early and late AGB phase. For this, the variation of flux density along the maxima, dust colour temperature profile of the region, mass of the gas in the nods and the possible direction of the mass loading have been extensively examined.

2   METHODS

We adopt the following method in order to study the dust structure around the white dwarf.

1.   We search 100 micron dust structure around hot white dwarfs.

2.   The past history of the evolution of white dwarfs will be studied by carefully examining the dust structure around the white dwarf.

3.   The interaction between the stellar wind in the post AGB phase will be studied.

4.   We intend to study the mass loading phenomena around the white dwarf.

We adopt the following methods to find the dust colour temperature of the region of interest and the mass of the gas in the selected region around the white dwarf.

2.1   TEMPERATURE ESTIMATION

We adopt the method developed by Schnee et al. (2005) to calculate the dust color temperature from the IRAS 60 micron and 100 micron flux densities. The temperature is determined by the ratio of the 60 micron and 100 micron flux densities. The dust temperature T_d in each pixel of a FIR image can be obtained by assuming that the dust in a single beam is isothermal and that the observed ratio of 60 micron to 100 micron emission is due to black body radiation from dust grains at T_d, modified by a power law emissivity spectral index. The flux density of emission at a wavelength ν, is given by

$$F_i = \left[\frac{2hc}{\frac{hc}{\lambda_i^3(e^{\lambda_i KT_d} - 1)}} \right] N_d a \lambda_i^{-\beta} \Omega_i$$

.... 1

where N_d represents column density of dust grains, α is a constant that relates the flux to the optical depth of the dust, β is the emissivity spectral index, and Ω_i is the solid angle subtended at λ_i by the detector. Following Dupac et al. (2003), we use the equation

$$\beta = \frac{1}{\delta + \omega T_d}$$ .... (2)

to describe the observed inverse relationship between temperature and emissivity spectral index. With the assumptions that the dust emission is optically thin at 60 micron and 100 micron and that $\Omega_w \approx \Omega_{100}$ (true for IRAS image), we can write the ratio, R, of the flux densities at 60 micron and 100 micron as

$$R = 0.6^{-(3+\beta)} \frac{e^{\frac{144}{T_d}} - 1}{\frac{240}{e^{T_d} - 1}}$$ .... (3)

Once the appropriate value of β is known, one can use Eq. (3) to derive T_d. The values of β depends on dust grain properties (composition, size, and compactness). For reference, a pure blackbody would have $\beta = 0$, the amorphous layer-lattice matter has $\beta \sim 1$, and the metals and crystalline dielectrics have $\beta \sim 2$. For a smaller value of Td, 1 can be dropped from both numerator and denominator of Eq. (3) and it takes the form

$$R = 0.6^{-(3+\beta)} \frac{e^{\frac{144}{T_d}}}{\frac{240}{e^{T_d}}}$$ .... (4)

Taking natural logarithm on both sides of Eq. (4) we find the expression for the temperature as

$$T_d = \frac{-96}{\ln\{Rx0.6^{-(3+\beta)}}$$ .... (5)

where R is given by

$$R = \frac{F\,(60\,\text{micron})}{f\,(100\,\text{micron})} \qquad \dots\dots\dots\dots (6)$$

F(60 micron) and *F*(100 micron) are the flux densities in 60 micron and 100 micron respectively.

2.2 MASS ESTIMATION

The dust masses are estimated from the infrared flux densities at 60 micron and 100 micron, following the analysis of Meaburn et al. 2000; Young et al., 1989, and Donofrio et al., 1999 (equation 7). The infrared flux can be measured from IRAS Sky-View images and images from the Groningen using both ALADIN2.5 and FITSVIEW2.0.1 softwares. The background subtraction is done by the averaging the background surrounding the object and multiplying by the number of pixels containing the object. The black body intensity can be calculated using the basic expression as given in equation (8). The resulting dust mass depends on the physical and chemical properties of the dust grains, the adopted dust temperature and the distance to the object:

$$m_{dust} = \frac{4}{3}\frac{\alpha\rho}{Qv}\left[\frac{SvD^2}{B(v,T)}\right] \qquad \dots\dots\dots\dots (7)$$

where, α = Weighted grain size, ρ = Grain density, Q_v = Grain emissivity, S_v = flux density. The Plank's function is a well known function, given by this equation,

$$B(v,T) = \frac{2hv^3}{c^2}\left[\frac{1}{\exp\left(\frac{hv}{KT}\right)-1}\right] \qquad \dots\dots\dots\dots(8)$$

It is clear from the expression (8) that the value of Plank Function [$B(v,T)$] for longer wavelength is higher than that of the shorter wavelength. Consequently, the range of $B(v,T)$ for fixed temperature goes narrower if wavelength of the images increases.

3. REGION OF INTEREST

We planned to study the region as shown in Fig. 1a. This region has one white dwarf, namely WD 1003-441 (see plus mark in Fig. 1). The position of this white dwarf is R.A.(J2000)= $10^h\,05^m\,24.37^s$

and Dec.(J2000)= -44° 21' 31.29".

Fig. 1: (a) 100 micron IRAS image of the region of interest. The symbol '+' represents the position of white dwarf WD 1003-441. (b) Contour maps showing the rounded filamentary nodes around the white dwarf.

4. RESULT & DISCUSSION

First we present the our results concerning the interaction between the stellar wind emitted from the post AGB phase of the white dwarf with the surrounding interstellar medium. The study of relative flux density helps us to know about the inner dynamics of the region. In addition, this study is useful to estimate the dust color temperature and the mass of the dust in the selected region. After getting information regarding the possible energy needed to make the structure, we calculate/estimate weather this amount of energy can be supplied by the white dwarfs or not.
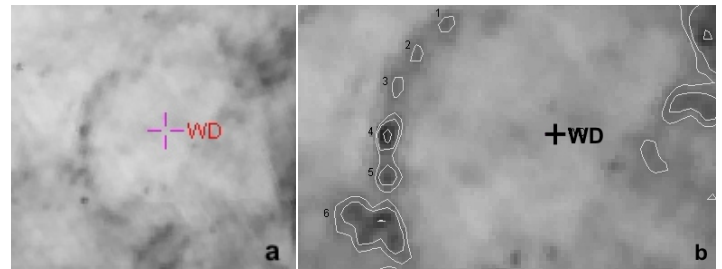

Fig. 2: (a) Region of interest (ROI) showing line joining the maxima of the nodes as shown in Fig. 1b. The optical image of the white dwarf is shown in the left. (b) The variation of relative flux density is plotted along the path, starting from top maxima, i.e., '1' to the bottom maxima i.e., '6'.

The studied region has one white dwarf, namely WD 1003-441. The position of this white dwarf is R.A.(J2000)= $10^h05^m24.37^s$ and Dec.(J2000)= 44°21'31.29". 100 micron IRAS image centered at R.A.(J2000)= $10^h04^m48.24^s$ and Dec.= -44°25'43.5" is shown in Fig. 1a. The position of the white dwarf is shown by the symbol '+'. In the northern part of white dwarf, grey shaded filamentary arc can be seen. The contour map of the image presented in Fig. 1b shows six maxima (represented by 1, 2, 3, 4, 5 and 6) from top to bottom. These maxima have 3 times greater values of relative flux density than that of the background. The minimum and maximum

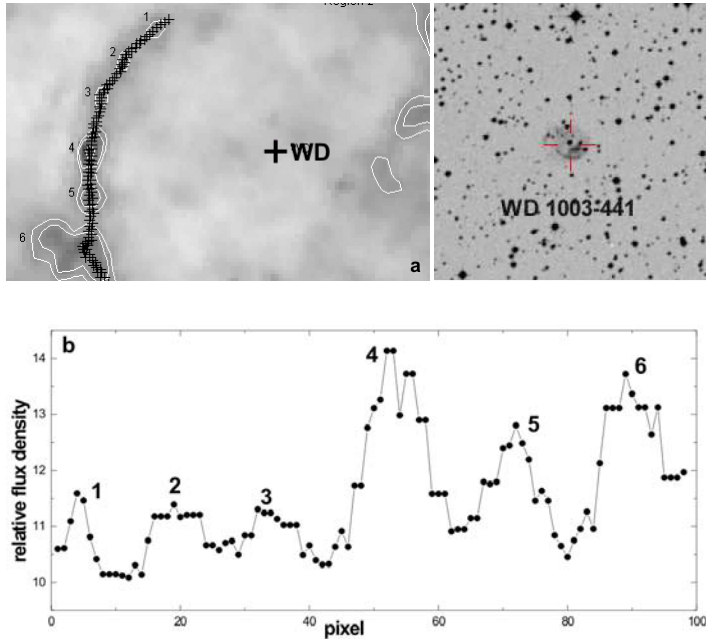relative flux density is found at maxima '4' and '6'.

Fig. 2a shows the path joining all the maxima from '1' to '6'. The path goes through 1 →2 → 3 →4 → 5 → 6 from top to bottom. The value of flux density is measured at all pixel on the path. Fig. 2b shows the variation of relative flux. The maximum relative flux density at '1', '2', and '3' are very nearly equal. Maxima '5' showed less flux than that of '4' and '6'. Interestingly it is found that the path joining the maxima 1 → 2 → 3 → 4 → 5 are point of perfect arc. Maxima '6' is somewhat deviated outward from the arc-like structure. It is noticed that the mass at '1', '2' and '3' are growing day by day in equal rate. It is also found that the separation between all the maxima is equal.

Star with initial masses between '1' and '9' solar masses that end up as white dwarf must lose a substantial fraction of their mass before they leave asymptotic giant branch (AGB). Most of the mass loss occurs near the end of AGB lifetime. These losses of mass are appear in the form of nodes around the white dwarf. As time passes, mass is found to be deposited rapidly around the white dwarf. To study the mass loading on the maxima, we joined the maxima of the infrared clouds and the white dwarf (see Fig. 3a). The variation of relative flux density along the path helps us to understand the mass loss pattern. Fig. 3a shows the line joining the maxima of the region (1, 2, 3, 4, 5 and 6) and white dwarf WD

1003-441. The regular ups and down in the flux density along the path indicate the continuous mass loading. The maxima `1' (Fig. 4.10b), `2' (Fig. 3c) and `4' (Fig. 3e) are found to unaffected due to the white dwarf. There are not any additional mass deposited in the path. The maxima '3' (Fig. 3d), '5' (Fig. 3f) and '6' (Fig. 3g) shows the continuous mass loading trend.
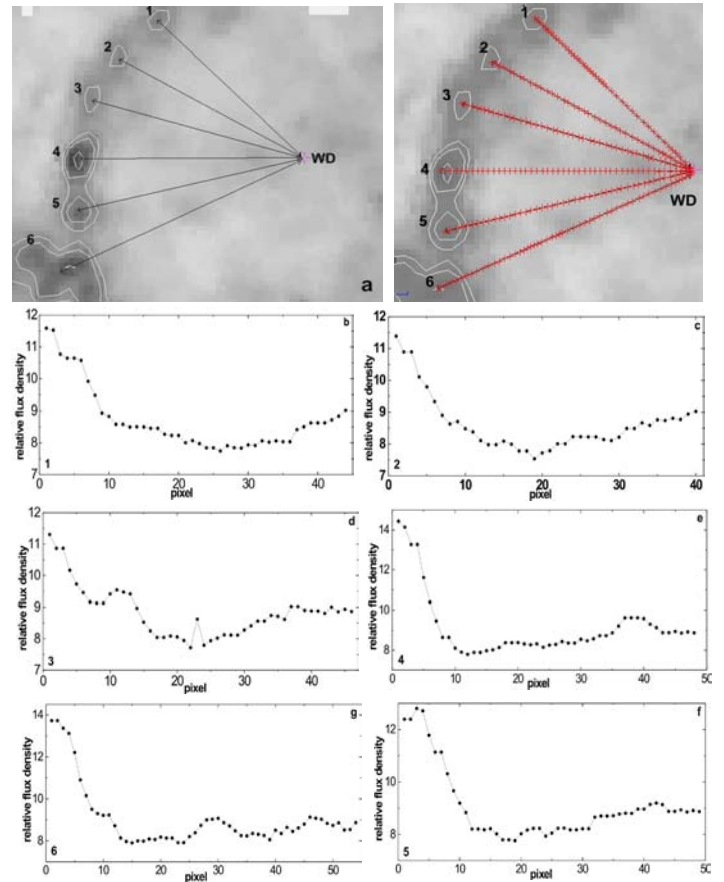

Fig. 3: Variation of relative flux density along straight line joining the maxima (1, 2, 3, 4, 5 and 6) and the white dwarf WD 1003-441. The image with our sketch is shown in (a) and the variation is shown in b, c, d, e, f and g. The first pixel in the plots begins from the respective maxima.

The most interesting mass loading has seen in the path joining '3' and the white dwarf (Fig. 3d). This path showed regular ups and downs in relative flux density. Similar mass loading trend is observed in the path joining '6' and white dwarf, but it showed relatively less mass-loading than that of '3'. The mass loading rate can be increased in the path as 2 → 1 → 4 → 5 → 6 → 3. In term

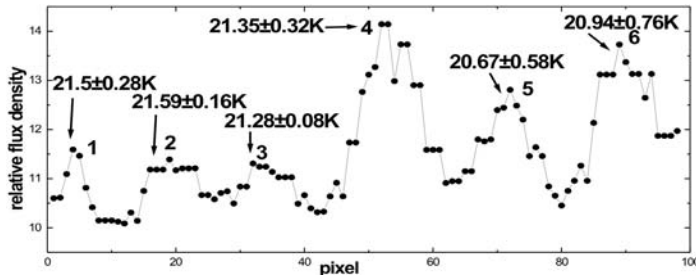of mass loading, the path '2' is most passive where as the path of `3' is most active.

Fig. 4: The variation of relative flux density is plotted along the path which connects the maxima 1 → 2 → 3 → 4 → 5 → 6. The maximum temperature at the maxima is shown.

To calculate the dust color temperature we used the 100 micron and 60 micron IRAS image in ALADIN2.5 software. It is found that there are very similar temperature in the maxima '1', '2', '3' and '4' (Fig. 4). Maxima '1', '2' and '3' has similar maximum relative flux density. The temperature in the maxima '1', '2', '3', '4', '5' and '6' are found to be 21.5 ± 0.28 K, 21.59 ± 0.16 K, 21.28 ± 0.08 K, 21.35 ± 0.32 K, 20.67 ± 0.58 K and 20.94 ± 0.76 K respectively. The maximum temperature is found at '2' where as the minimum temperature is at '5'. Maxima '6' has high value of flux density but has low temperature than that of other maxima '1', '2', '3' and '4'. Similar temperature in the maxima '1', '2', '3' and '4' shows their temperature are increasing in similar manner. The maxima can be arranged in increasing order of temperature as $5 \rightarrow 6 \rightarrow 3 \rightarrow 4 \rightarrow 1 \rightarrow 2$.

The mass of the dust is estimated using Henning et al. (Eq. 7). The value of their respective temperature is used in order to calculate the value of the plank function (Eq. 8). We used 100 micron IRAS image for the mass estimation. The region '6' is found to be the massive region. It has the mass (80.9 ± 19.8) x 10^{-3} solar masses. The second and third massive region is found to be region '4' and region '5' where masses were (21.7 ± 2.2) x 10^{-3} and (13.6 ± 2.6) x 10^{-3} solar masses, respectively. The mass of the fourth and fifth nodes (region '3' and region '1') are found where masses are (6.7 ± 0.2) x 10^{-3} and (6.0 ± 0.5) x 10^{-3} solar masses. The region '2' is least: (5.7 ± 0.8) x 10^{-3} solar mass. These are background

corrected values. Total mass is about 0.134 ± 0.019 solar masses. This amount of mass can be contributed by the white dwarf WD 1003-441.

In the optical (red) wavelength, the surface brightness of this white dwarf is low. The spectral index of this white dwarf in V band is 16.60 (McSion & Cook 2003). So, this white dwarf is relatively hot. WD 1003-441 is a PG1159 star with 9-11 detected periods and an associated planetary nebula mass ejection (SIMBAD database). Thus, this white dwarf is still ejecting envelops of helium flashes. This can be seen in the figure.

We conclude that the curved structure in the region of interest is formed probably due to the interaction between the ambient interstellar medium and the He flashes of the parent planetary nebula of the white dwarf WD 1003-441. The total mass of the filamentary arc is found to be ~ 8 x 10^{-2} solar masses, which is quite reasonable. The mass loss rate of the post AGB star goes up to 10^{-5} solar masses/year. This means that the first He flash possibly occurred at least ~ 1000 years ago.

5.   CONCLUSION

We studied the 100 micron dust structures around white dwarf WD 1003-441. The post Asymptotic Giant Branch (AGB) emission of white dwarf's precursors' wind and the ambient interstellar matter is thoroughly studied. For this, distribution of the relative flux density of each pixel of the images are analyzed in the context of the dust color temperature, mass loading trend and the amount of total mass deposited due the interaction in the interstellar medium. The 100 micron far infrared image is provided by the Groningen server of Infrared Astronomical Satellite (IRAS) survey. The spectral index of the white dwarf was taken from McSion & Cook (2003). These images were processed in the image reduction software ALADIN2.5. The calculations for the dust color temperature (Schnee et al. 2005 & Dupac et al., 2003) and the mass (Young 1989) were carried out using 100 micron IRAS image.

The curved emission structure at 100 micron in the region of interest B is due to the interaction between the ambient interstellar

medium and the He-flashes of the parent planetary nebula of the central star, i.e., white dwarf WD 1003-441. This white dwarf is neither relatively hot. WD 1003-441 is a PG1159 star with 9-11 detected periods and an associated planetary nebula mass ejection. The maximum and minimum dust color temperature of the dust structure is found to be 22.0 K to 20.0 K. The total mass of the filamentary arc is found to be ~ 8 x 10^{-2} solar masses, which is quite reasonable. The mass loss rate of the post AGB star goes up to 10^{-5} solar masses/year. This means that the first He-flash occurred at least ~ 1000 years ago. Thus, envelops of helium flashes are still spherically symmetric here.

6.   ACKNOWLEDGEMENTS

References

Aryal, B., Weinberger, R.A., 2006. Journal Astronomy & Astrophysics **245**, 306.

Aryal, B., Rajbahak R., Weinberger, R.,2010. Monthly Notice of Royal Astronomical Society, **402**, 1307.

Aryal, B., Rajbahak R., Weinberger, R., 2009. Astrophysics & Space Science, **223**.

Balick, B., 2002. Astronomy & Astrophysics **282**, 143.

Blandford, R.D., Rees M.J., 1974. Monthly Notice of Royal Astronomical Society **169**, 395.

Cox, D.P., 2005 Astronomy & Astrophysics **43**, 237.

Donofrio, et.al., 1999. Astronomy & Astrophysics Supp. **105**, 12.

Dupac, X., et al., 2003. Publication Astron. Society Asia Pacific **115**, 965.

http: //simbad.u-strasbg.fr **(SIMBAD)**

http: //skyview.gsfc.nasa.gov **(SKYVIEW)**

McSion M., Cook S. M., 2003. Catalog of WD, Groningon .

Meaburn, et.al., 2000. Astronomy & Astrophysics **215**, 903.

Rees, M.J., 1984. Annu. Rev. Astron. & Astrophysics **22**, 471.

Schnee, S.L., Naomi A. R., Alyssa A. G. et al., 2005. Astrophysical Journal **634**, 442.

Young, 1989. Astrophysical Journal **109**, 725.